Int. J. Therm. Sci. (2000) 39, 797–805

S1290-0729(00)00271-4/FLA

Parametric study of natural convection heat transfer from horizontal rectangular fin arrays

Senol Baskaya *, Mecit Sivrioglu, Murat Ozek

Gazi University, Faculty of Engineering and Architecture, Department of Mechanical Engineering, 06570 Maltepe, Ankara, Turkey

(Received 23 July 1999, accepted 10 January 2000)

Abstract—A systematic theoretical investigation of the effects of fin spacing, fin height, fin length and temperature difference between fin and surroundings on the free convection heat transfer from horizontal fin arrays was carried out. The three-dimensional elliptic governing equations were solved using a finite volume based computational fluid dynamics (CFD) code. Preliminary simulations were made for cases reported in the literature. After obtaining a good agreement with results from the literature a large number of runs were performed for a detailed parametric study. It has been shown that it is not possible to obtain optimum performance in terms of overall heat transfer by only concentrating on one or two parameters. The interactions among all the design parameters must be considered. Results are presented in graphical form together with optimum values and correlations, and compared with available experimental data from the literature. © 2000 Éditions scientifiques et médicales Elsevier SAS

natural convection / fin arrays / computational fluid dynamics / parametric study / heat transfer

Nomenclature

a, d	correlation constants	
A	area	m^2
g	acceleration due to gravity	$m\cdot s^{-2}$
h	$= Q/(A\Delta T)$, heat transfer coefficient	$W\cdot m^{-2}\cdot K^{-1}$
H	fin height	mm
k	thermal conductivity	$W\cdot m^{-1}\cdot K^{-1}$
L	fin length	mm
Nu_S	$= hS/k$, Nusselt number based on S	
Nu_L	$= hL/k$, Nusselt number based on L	
Pe	$= Re\,Pr$, Peclet number	
P_m	motion pressure	Pa
Pr	Prandtl number	
Re	Reynolds number	
Q	heat transfer rate	W
Ra_S	$= g\beta(T_F - T_a)S^3/(\nu\alpha)$, Rayleigh number based on S	
Ra_L	$= g\beta(T_F - T_a)L^3/(\nu\alpha)$, Rayleigh number based on L	
S	fin spacing	mm
T	temperature	°C
u, v, w	velocity components	$m\cdot s^{-1}$
x, y, z	Cartesian coordinates	

Greek symbols

α	thermal diffusivity	$m^2\cdot s^{-1}$
β	coefficient of thermal expansion	K^{-1}
Δ	difference	
ν	kinematic viscosity	$m^2\cdot s^{-1}$
ρ	density	$kg\cdot m^{-3}$

Subscripts

a	ambient
b	fin base
F	fin
L	fin length
opt	optimum value
S	fin spacing

1. INTRODUCTION

Needs for buoyancy driven ventilation appear in a variety of engineering applications, ranging from cooling of electronic components and solar energy applications to cooling of nuclear reactor fuel elements. For an efficient application of natural convection to cooling processes

* Correspondence and reprints.
baskaya@mikasa.mmf.gazi.edu.tr

it is necessary to fully understand the mechanisms involved. In the free-convection cooling of electronic and thermoelectric devices, as well as in improving the heat transfer in radiators for air conditioning and in other heat exchangers, finned surfaces are being extensively used. Compared to a bare plate, a finned surface increases the heat transfer area. However, with the fins the flow rate is reduced. Hence, if not properly designed it is possible that no improvement is achieved in terms of overall heat transfer. Therefore, only if the fins are properly designed, they are very attractive for these applications since they offer an economical, trouble-free solution to the problem.

In spite of the fact that the heat transfer from fins has been the subject to numerous experimental and theoretical investigations, few systematic parametric studies can be found in the literature. An extensive review and discussion of work done on the convective heat transfer in electronic equipment cooling was presented by Incropera [1], summarizing various convection cooling options. A great number of analytical and experimental work has been carried out on this problem since Elenbaas [2] first introduced the problem of natural convection between vertical parallel plates. One of the earliest studies of the heat transfer from fin arrays is that of Starner and McManus [3] who presented heat transfer coefficients for four differently dimensioned fin arrays with the base vertical, 45 degrees and horizontal. They showed that incorrect application of fins to a surface actually may reduce the total heat transfer to a value below that of the base alone. A similar experimental study was conducted by Welling and Woolbridge [4] on rectangular vertical fins. They reported optimum values of the ratio of fin height to spacing. In the previous two studies the fin length was constant. Average heat transfer coefficients and flow field observations were presented by Harahap and McManus [5] for two different fin lengths. They also reported correlations representing all their experimental data by making use of nondimensional numbers and all the relevant dimensions of fins. From flow pattern observations they conclude that the single chimney flow pattern yields higher rates of heat transfer. Jones and Smith [6] studied the variations of the local heat transfer coefficient for isothermal vertical fin arrays on a horizontal base over a wide range of fin spacings. A simplified correlation, an optimum arrangement for maximum heat transfer and a preliminary design method were suggested. For a wide range of temperatures, Rammohan and Venkateshan [7] made an interferometric study of heat transfer by free convection and radiation from a horizontal fin array. Correlations useful for thermal design were presented. The authors stressed the importance of the mutual interaction between free convection and radiation. Recently, an experimental investigation was carried out by Yüncü and Anbar [8] on natural convection heat transfer from rectangular fin arrays on a horizontal base for effects due to fin spacing, fin height and temperature difference between fin base and surroundings. Optimum fin spacing values and a correlation were reported. However, results are only for a fixed fin length and fin thickness. One of the first numerical studies on this subject was carried out by Sane and Sukhatme [9]. Governing equations were solved numerically using a finite difference technique. They obtained good agreement with experimental data. In addition, flow visualization studies were carried out in order to depict the zone in which the single chimney pattern occurs. A great number of investigations on this subject has also been made in the form of Ph.D. dissertations, see, for example, Shalaby [10] and Tikekai [11].

The present work investigates the effects of a wide range of geometrical parameters to the heat transfer from horizontal fin arrays. Effects due to changes in fin spacing, fin height, fin length and temperature difference between fin and surroundings are investigated together, hence, preventing mistakes possible due to incorrect assumptions and usage of a constant value for one of the geometrical parameters.

2. NUMERICAL MODEL

A schematic drawing of the fin array under investigation is shown in *figure 1* together with the actual simulated part of one fin. An infinite number of fins with

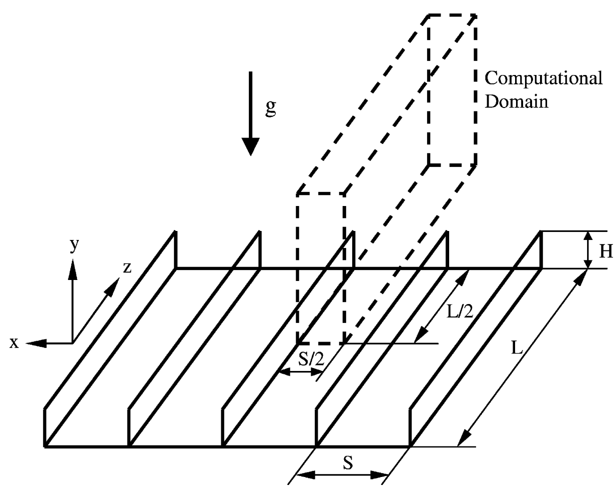

Figure 1. Schematic drawing of the fin array under investigation.

negligible thickness was assumed. The fin surfaces and fin array base were assumed to be at a uniform temperature. Laminar natural convection is the mechanism for heat transfer from the fin array. Radiation heat loss is neglected. As can be seen from *figure 1*, the computational domain was reduced to one quarter of one fin channel with an extension towards one open end, in agreement with the geometry and symmetry conditions of the problem. A detailed description of the theoretical approach undertaken is given below.

3. GOVERNING EQUATIONS

The natural convection flow under investigation was modeled by a set of elliptic partial differential equations describing the conservation of mass, momentum and energy in three rectangular Cartesian coordinate directions:

- conservation of mass:

$$\frac{\partial(\rho u)}{\partial x} + \frac{\partial(\rho v)}{\partial y} + \frac{\partial(\rho w)}{\partial z} = 0 \tag{1}$$

- conservation of momentum:

$$\frac{\partial(\rho u^2)}{\partial x} + \frac{\partial(\rho uv)}{\partial y} + \frac{\partial(\rho uw)}{\partial z} = -\frac{\partial(P_\mathrm{m})}{\partial x} + \rho\nu\left(\frac{\partial^2 u}{\partial x^2} + \frac{\partial^2 u}{\partial y^2} + \frac{\partial^2 u}{\partial z^2}\right) \tag{2}$$

$$\frac{\partial(\rho vu)}{\partial x} + \frac{\partial(\rho v^2)}{\partial y} + \frac{\partial(\rho vw)}{\partial z} = -\frac{\partial(P_\mathrm{m})}{\partial y} + \rho\nu\left(\frac{\partial^2 v}{\partial x^2} + \frac{\partial^2 v}{\partial y^2} + \frac{\partial^2 v}{\partial z^2}\right) + g(\rho - \rho_\mathrm{a}) \tag{3}$$

$$\frac{\partial(\rho wu)}{\partial x} + \frac{\partial(\rho wv)}{\partial y} + \frac{\partial(\rho w^2)}{\partial z} = -\frac{\partial(P_\mathrm{m})}{\partial z} + \rho\nu\left(\frac{\partial^2 w}{\partial x^2} + \frac{\partial^2 w}{\partial y^2} + \frac{\partial^2 w}{\partial z^2}\right) \tag{4}$$

- conservation of energy:

$$\frac{\partial(\rho uT)}{\partial x} + \frac{\partial(\rho vT)}{\partial y} + \frac{\partial(\rho wT)}{\partial z} = \frac{\nu}{Pr}\left(\frac{\partial^2 T}{\partial x^2} + \frac{\partial^2 T}{\partial y^2} + \frac{\partial^2 T}{\partial z^2}\right) \tag{5}$$

In the above equations it is apparent that the Boussinesq approximation has not been applied. Gray and Giorgini [11] showed that the error due to using the Boussinesq approximation is less than 10 % for air as long as $\Delta T \le 28.6\,°\mathrm{C}$. However, in the present simulations the temperature differences are up to 100 °C, hence, the Boussinesq approximation was not employed.

The assumptions employed in the governing equations are in agreement with steady, incompressible, laminar flow of air with constant properties, except for density which is taken as a function of temperature only, $\rho = \rho(T)$. Radiation heat transfer is neglected. The reference density ρ_a was calculated from the inlet temperature. The change in the Pr number with temperature was found to be negligible and a constant value of $Pr = 0.70$ was used.

3.1. Solution algorithm

The numerical model is based on a control volume–finite difference formulation. The above equations are integrated over each control volume to obtain a set of discretized linear algebraic equations of the form

$$a_P\phi_P = \sum a_{\mathrm{nb}}\phi_{\mathrm{nb}} + b \tag{6}$$

Equations in the format given above are called finite volume equations. Finite volume equations describe processes affecting the value of ϕ in cell P in relation to its neighbor cells together with the source term b. These equations were solved by the widely used commercial CFD package PHOENICS (Rosten and Spalding [13]) employing the SIMPLEST algorithm (Spalding [14]) for the pressure correction process along with the solution procedure for the hydrodynamic equations. The package uses a staggered grid arrangement. Implicit temporal differencing is employed and, for the discretization of convective–diffusive transport, the hybrid scheme is the default scheme within the code (see Patankar [15] for details). This scheme combines the stability of the upwind-scheme with the approximation accuracy of the central-difference-scheme. In the hybrid-scheme, diffusion is cut off when the cell Peclet number ($Pe = Re\,Pr$, i.e. the ratio of heat convection to heat conduction) equals 2.0. In other words, the convective transport is assumed to dominate diffusive transport, and the hybrid-scheme reduces to the upwind formulation, with diffusion terms being neglected. The central-difference-scheme leads to a second-order truncation error in the approximations, whereas the upwind-scheme gives only first-order accuracy. The discretized equations are solved by the TDMA (Tri-Diagonal-Matrix-Algorithm). The same technique has been successfully applied before by Baskaya et al. [16] to a much more complex natural convection problem.

3.2. Boundary conditions

All boundary conditions were implemented by the inclusion of additional source and/or sink terms in the finite volume equations for computational cells at the boundaries. In natural convection flows there is no information regarding the velocity and temperature fields before the start of calculations. Since governing equations are invariably coupled, the temperature field causes the velocity field to develop and in turn the velocity field affects the temperature field with the promotion of convective heat transfer. *Figure 1* shows the horizontal fin array under investigation with the coordinate system used and the relevant dimensions. The computational domain is also shown on this figure. Because only one fin channel is investigated and because of symmetry conditions only one quarter of this fin is simulated. The simulated part is shown in *figure 2* in more detail. One can see that the computational domain has been extended beyond the actual dimensions of the fin array in order to account for effects due to the surrounding of the fin array.

The imposed boundary conditions were as follows. The fin surface and base were held at a constant temperature T_F (*ABEFA* and *BCDEB* surfaces). Symmetry boundary conditions were applied at *AFEHJKA*, *BCLKB* and *CGILC*. All the remaining boundaries were open boundaries where air enters the channel at the ambient temperature T_a and corresponding density ρ_a. Here the ambient pressure was used as a stagnation boundary condition with the incoming mass having the ambient temperature. The static pressure was assumed equal to the pressure of the surrounding atmosphere. Molecular (laminar) transport boundary conditions were applied to the fin walls to simulate the effects of laminar friction and heat transfer, known as no-slip boundary conditions.

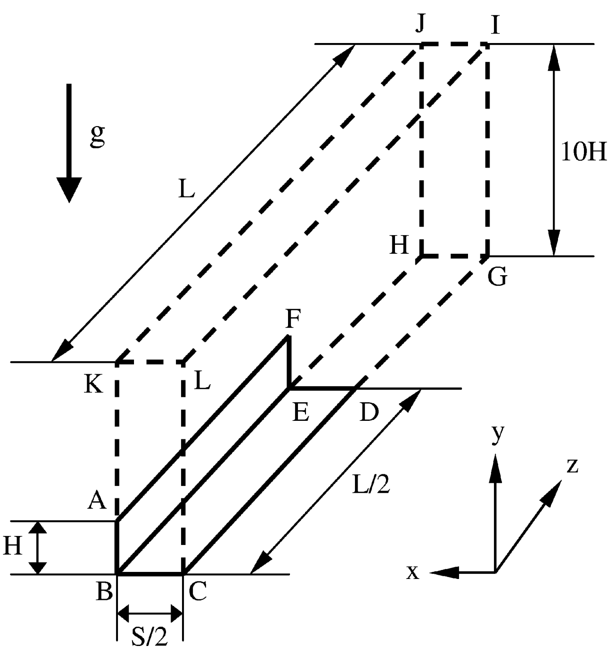

Figure 2. Schematic drawing of the computational domain with locations of the applied boundary conditions.

3.3. Convergence and grid independency

Due to the iterative process of the code, convergence was used as the monitor of achievement of the final solution. The criterion of convergence of the numerical solution is based on the absolute normalized residuals of the equations that were summed for all cells in the computational domain. Convergence was considered as being achieved when these residuals became less than 10^{-3}, which was the case for most of the dependent variables. Iterative convergence was also checked by terminating the solution only then progressive single cell values of pressure, velocity and temperature showed little change per iteration as the calculation progressed. Furthermore, checks for the achievement of a final solution were made on the basis of the conservation of mass, momentum and energy. The maximum acceptable error in the global heat, mass and momentum balances was less than 5 %.

Grid independency checks were made and the final simulations were achieved with cell numbers ranging from $6 \times 10 \times 40$ to $8 \times 30 \times 40$ in the x–y–z coordinate directions, depending on the actual physical dimensions used. Coarser grid distributions were not able to give accurate results in agreement with data from the literature. False time step relaxation for the three velocity components and temperature, and linear relaxation for pressure was used to obtain more rapid convergence. The simulations exhibited divergence if no relaxation was applied.

4. RESULTS, COMPARISONS AND DISCUSSION

The mechanism of the flow in this type of fin array is complicated, hence, it is difficult to obtain physically meaningful solutions. Therefore, before the start of the parametric study, trial simulations were conducted for the verification of the computational domain and numerical procedures applied. *Figure 3* compares present results with experimental data by Harahap and McManus [5].

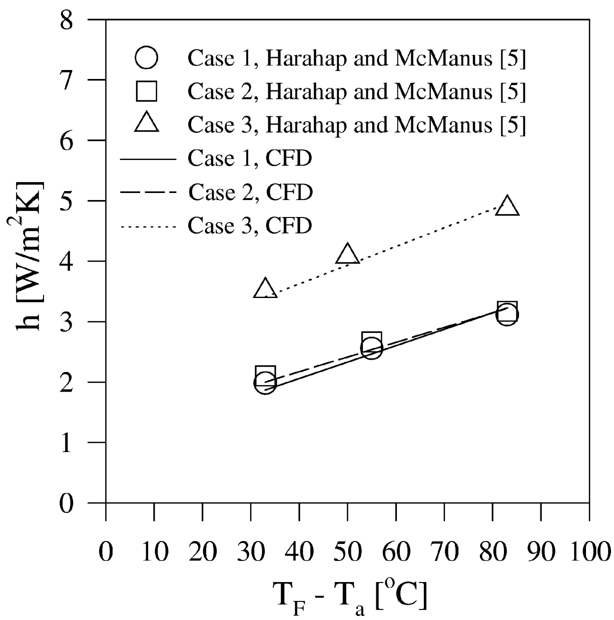

Figure 3. Validation of the computational approach: present CFD results compared with experimental data by Harahap and McManus [5].

Case 1 is for $L = 254$ mm, $H = 25$ mm, $S = 8$ mm; case 2 is for $L = 254$ mm, $H = 6.3$ mm, $S = 6.4$ mm and case 3 is for $L = 127$ mm, $H = 38$ mm, $S = 6.4$ mm. As can be seen from the figure, present numerical results are in very good agreement with experimental values. The maximum difference between experimental and CFD values is 8 %.

After the above presented trial runs, a systematic parametric study was conducted. Solutions were obtained for the following range of values: $L = 127$–381 mm, $S = 4$–38.1 mm, $H = 6.3$–50 mm, $H/L = 0.018$–0.370, $T_F - T_a = 33$–100 K and $Ra_S = 2.1{\cdot}10^2$–$1.8{\cdot}10^5$. However, before presenting and discussing results from this parametric study it is important to understand the general flow patterns dominating flows from fin arrays. Flow patterns due to buoyancy forces acting on the surrounding fluid of vertical fins are of a chimney type. *Figure 4* shows the generally observed single chimney type flow pattern. The surrounding fluid enters the fin region from the two open ends and develops a vertical component of velocity as the air is heated. The resulting chimney being only a fraction of the width of the fin array. In certain cases the single chimney breaks up into several smaller chimneys as shown in *figure 5*. Here, the main inflow is again from the open ends, however, several chimneys can form and hence certain regions above the fin can consist of downward flows. Single chimneys are more efficient in the heat removal compared to multiple

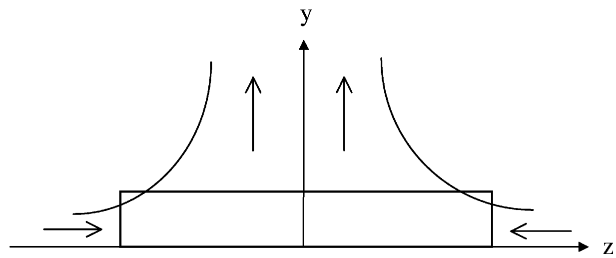

Figure 4. Single chimney type flow pattern.

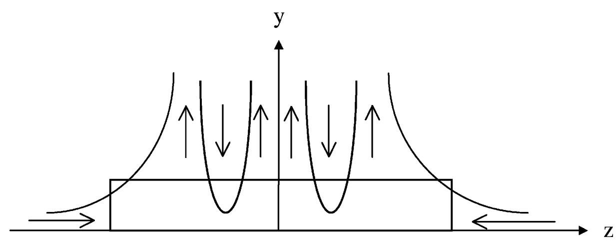

Figure 5. Multiple chimney type flow pattern.

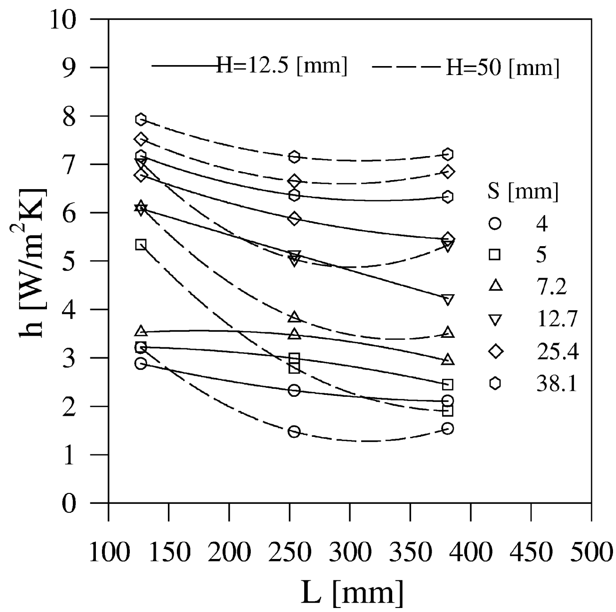

Figure 6. Variations of the heat transfer coefficient h with fin length for different values of fin spacing and fin height.

chimneys. With these different flow configurations in mind, results presented below can be understood more easily.

Figure 6 presents variations of the heat transfer coefficient h with fin length for different values of fin spacing and fin height. On the overall, the value for the heat transfer coefficient reduces with fin length. This is due to

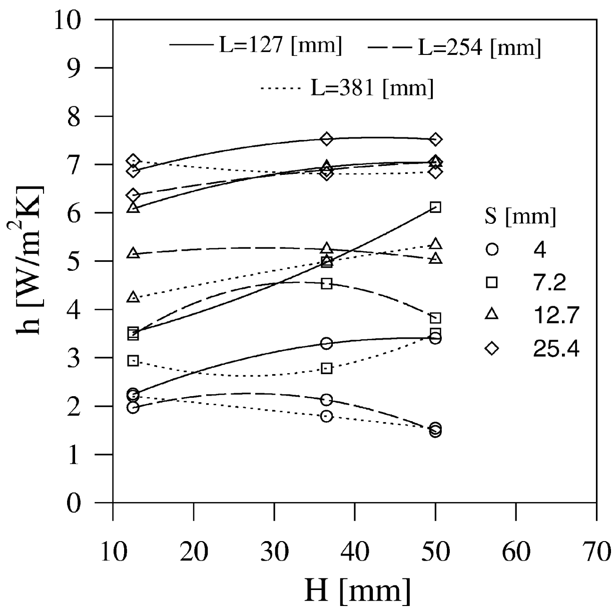

Figure 7. Effects of variations in fin height on the heat transfer coefficient for different fin length and fin spacing values.

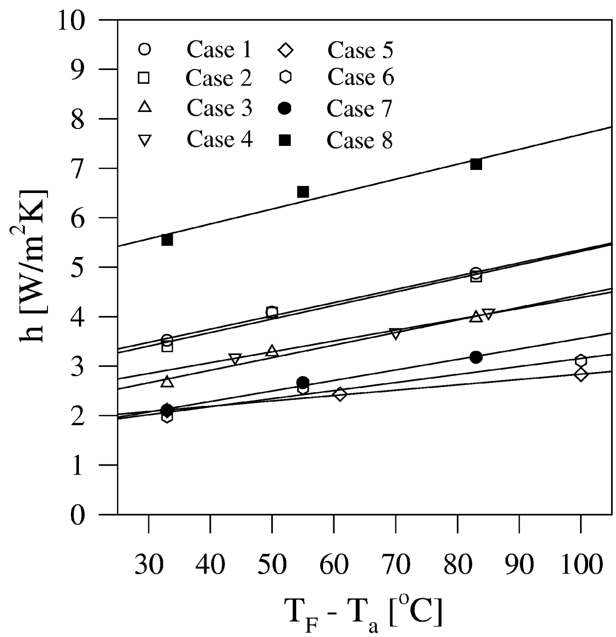

Figure 8. Changes in the heat transfer coefficient due to variations in the temperature difference between the fin surface temperature and the ambient temperature, for different geometrical dimensions.

variations in the flow patterns. Shorter fins produce more dominant single chimney flows with higher rates of heat transfer. On the other hand, multiple chimneys are present for long fins.

Effects of variations in fin height on the heat transfer coefficient are shown in *figure 7* for various fin spacings and fin lengths. On the overall, the heat transfer coefficient values do increase with increase in the fin height. Although a small drop with increase in the fin height was calculated for the smallest fin spacing. However, one can see that it is very difficult to draw clear conclusions due to the various parameters involved.

Results of heat transfer coefficient values for various temperature difference values $T_F - T_a$ between the fin surface temperature T_F and the ambient temperature T_a are shown in *figure 8* for different geometric cases. The cases studied are given in *table I*.

From *table I* and *figure 8* it can be seen that effects due to two different values of fin lengths are studied for different values of fin height and fin spacing. In the figure results for a flat plate are also shown for comparison. For all the cases the heat transfer coefficient increases with the increase in the temperature difference. In addition, the increase rates are also similar. However, one can see that shorter fins with greater heights yield larger values of the heat transfer coefficient.

The spacing S between fins plays a vital role in the heat transfer process of fin arrays. *Figures 9–11* show

TABLE I
Geometrical dimensions for the cases investigated in *figure 8*.

Case number	L [mm]	H [mm]	S [mm]
1	127	38	6.3
2	127	25	8
3	127	13	6.3
4	127	6.3	6.3
5	254	38	6.3
6	254	25	8
7	254	6.3	6.3
8	flat plate		

how Q/A_b is affected by variations in the fin spacing. Also shown on these figures are variations due to changes in the H/L ratio. The figures are for $L = 127$ mm, $L = 254$ mm and $L = 381$ mm, respectively. Comparison of all three figures with respect to fin length shows that Q/A_b values reduce with increase in the fin length. The reason for this is the change of the flow characteristic from a single chimney type to a multiple chimney flow pattern with increasing fin length. Effects due to fin spacing and H/L ratio are very small in the lower range of H/L values, where only small changes are visible with increasing fin spacing. This is due to the fact that for low values of H/L the geometry approaches to that of a

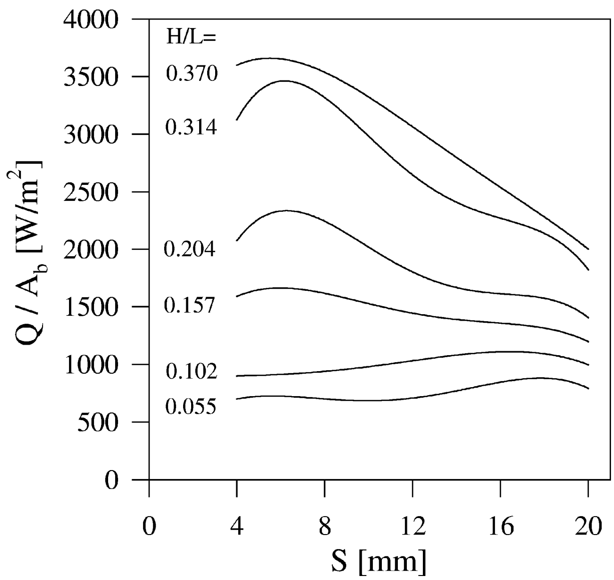

Figure 9. Effects of fin spacing and fin height to fin length ratio on heat transferred per unit base area, $L = 127$ mm.

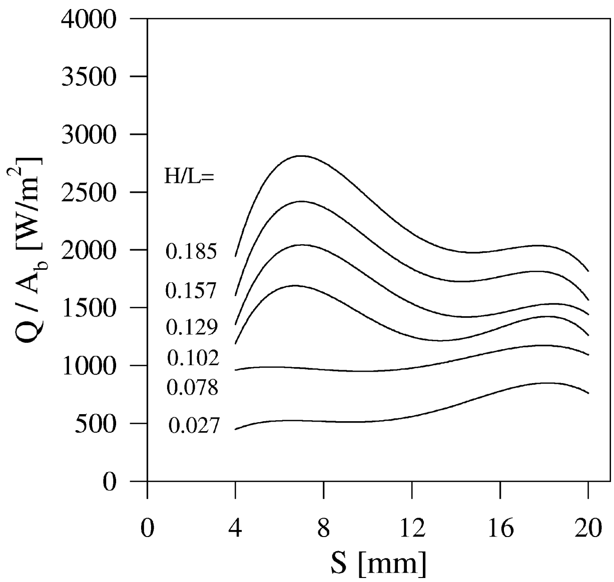

Figure 10. Effects of fin spacing and fin height to fin length ratio on heat transferred per unit base area, $L = 254$ mm.

flat plate. However, for large values of the H/L, changes with fin spacing are much more conclusive. Optimum fin spacings can be calculated for $L = 127$ mm and $L = 254$ mm, whereas for $L = 381$ mm an optimum value is not obvious to determine. Optimum fin spacings for $L = 127$ mm and $L = 254$ mm are found to be $S_{\text{opt}} \cong 6$ and 7 mm, respectively.

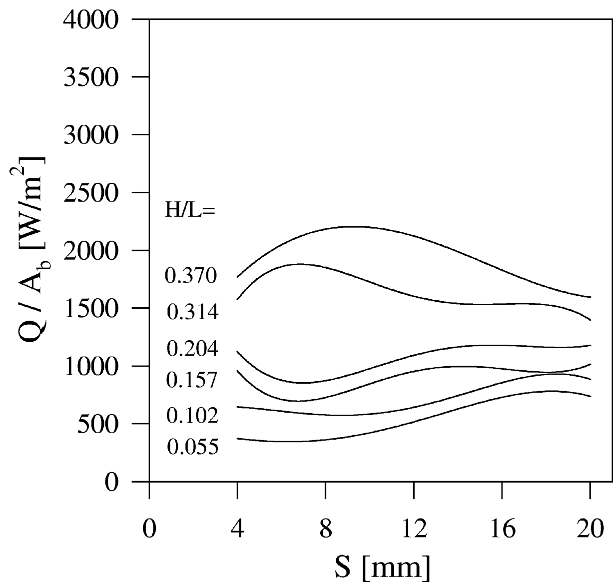

Figure 11. Effects of fin spacing and fin height to fin length ratio on heat transferred per unit base area, $L = 381$ mm.

Quantitative comparisons of present computational results with data from the literature are presented next. Nondimensional numbers used in the comparisons are explained first. Appropriate to natural convection heat transfer, results are presented in terms of an overall average Nusselt number, *Nu*, and a Rayleigh number, *Ra*, using S or L as the characteristic dimensions as defined below:

$$Nu_S = \frac{hS}{k}, \qquad Nu_L = \frac{hL}{k} \tag{7}$$

$$Ra_S = \frac{g\beta(T_{\text{F}} - T_{\text{a}})S^3}{\nu\alpha}, \qquad Ra_L = \frac{g\beta(T_{\text{F}} - T_{\text{a}})L^3}{\nu\alpha} \tag{8}$$

The heat transfer coefficient h is defined by the relation $h = Q/(A\Delta T)$. The thermophysical properties in the Nusselt and Rayleigh numbers were all evaluated at the film temperature $(T_{\text{F}} + T_{\text{a}})/2$.

Figure 12 presents overall Nusselt numbers for a range of Rayleigh numbers. Various cases are presented where fin height and fin length were changed. As can be seen from the data points plotted from the present simulations, the differences between the various cases are very small for high *Ra* numbers, but somehow more distinct for smaller *Ra* numbers. In order to compare present results with data from the literature a best fit line for all the numerical results was obtained. This best fit is compared with the data reported by Jones and Smith [6]. The overall trends are the same. The agreement is very good for

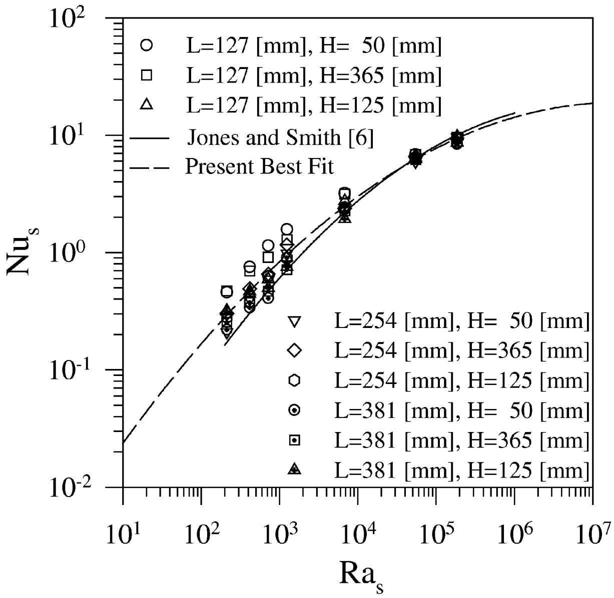

Figure 12. Authors' data and best fit to this data compared with recommended correlation of average free convection heat transfer data using fin spacing S as the characteristic dimension by Jones and Smith [6].

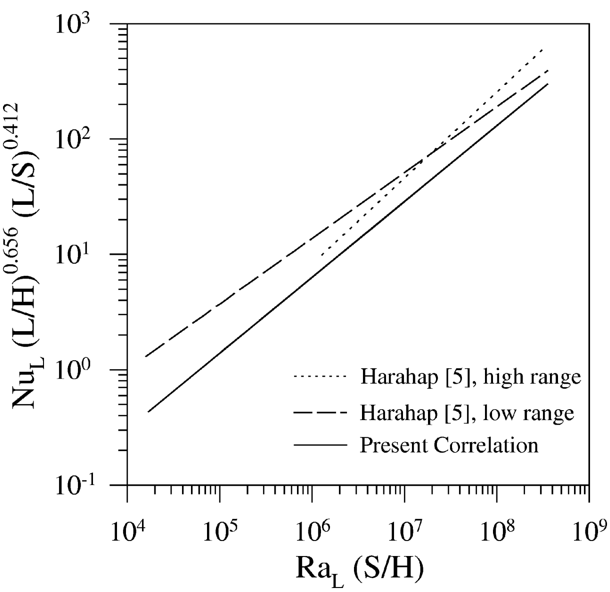

Figure 13. Correlation obtained from the present study compared with correlations proposed by Harahap and McManus [5].

higher *Ra* numbers but there is a small discrepancy in the lower *Ra* number range.

The same data as presented in *figure 12* was used to recalculate the data for *figure 13* where effects due to fin spacing, height and length are included in the *Nu* and *Ra* numbers, yielding a correlation as recommended by Harahap and McManus [5] in the following general form:

$$Nu_L = a\left[Ra_L\,\frac{S}{H}\right]^d\left(\frac{S}{L}\right)^{0.656}\left(\frac{H}{L}\right)^{0.412} \qquad (9)$$

where a and d are correlation constants. *Figure 13* compares the correlation obtained from the present study with correlations reported by Harahap and McManus [5] for two ranges of *Ra* numbers. The correlation constants reported by Harahap and McManus [5] are $a = 0.00522$ and $d = 0.57$ for the low range of *Ra* numbers and $a = 0.0002787$ and $d = 0.745$ for the high range. Correlation constants from the present study were found as $a = 0.00071561$ and $d = 0.6576$. *Figure 13* as well as the correlation constants show that present results are close to experimental measurements reported by Harahap and McManus [5].

5. CONCLUSIONS

The flow around and heat transfer from horizontal fin arrays were determined numerically using a finite volume based computational fluid dynamics (CFD) code. A large number of runs were carried out for a systematic theoretical investigation of the effects of fin spacing, fin height, fin length and temperature difference between fin and surroundings on the heat transfer processes involved. This study has shown that each of the variables of fin spacing, height, length and temperature difference produces an effect on the overall heat transfer. As a whole, we can conclude that the overall heat transfer is enhanced with increase in H, the height of the fin and decrease in L, the length of the fin, hence increase in H/L. In addition, for maximum heat transfer optimum values of S, the fin spacing were obtained.

Results from the present theoretical analysis clearly show that more experimental studies are needed in order to produce the most general and valid optimum design procedures. However, in experimental studies any of the dimensions should not be fixed, on the contrary, all dimensions should be varied, in order to yield a comprehension of all interrelated effects among all the relevant parameters.

REFERENCES

[1] Incropera F.P., Convection heat transfer in electronic equipment cooling, J. Heat Tran. 110 (1988) 1097–1111.

[2] Elenbaas W., Heat dissipation of parallel plates by free convection, Physica 9 (1942) 1–28.

[3] Starner K.E., McManus Jr.-H.N., An experimental investigation of free-convection heat transfer from rectangular-fin arrays, J. Heat Tran. (August 1963) 273–278.

[4] Welling J.R., Woolbridge C.B., Free convection heat transfer coefficients from rectangular vertical fins, J. Heat Tran. (November 1965) 439–444.

[5] Harahap F., McManus Jr.-H.N., Natural convection heat transfer from horizontal rectangular fin arrays, J. Heat Tran. (February 1967) 32–38.

[6] Jones C.D., Smith L.F., Optimum arrangement of rectangular fins on horizontal surfaces for free-convection heat transfer, J. Heat Tran. (February 1970) 6–10.

[7] Rammohan Rao V., Venkateshan S.P., Experimental study of free convection and radiation in horizontal fin arrays, Int. J. Heat Mass Tran. 39 (1996) 779–789.

[8] Yüncü H., Anbar G., An experimental investigation on performance of rectangular fins on a horizontal base in free convection heat transfer, Heat Mass Tran. 33 (1998) 507–514.

[9] Sane N.K., Sukhatme S.P., Natural convection heat transfer from horizontal rectangular fin arrays, in: Proc. of 5th International Heat Transfer Conference, Tokyo, Japan, 1974, Vol. 3, NC3.7, pp. 114–118.

[10] Shalaby M.A.I., Natural convection heat transfer from rectangular fin arrays, Ph.D. Thesis, I.I.T. Mumbai, India, 1983.

[11] Tikekai A.N., Comprehensive studies on natural convection heat transfer from vertical fin arrays, Ph.D. Thesis, Shiraji University, India, 1996.

[12] Gray D.D., Giorgini A., The validity of the Boussinesq approximation for liquids and gases, Int. J. Heat Mass Tran. 19 (1976) 545–551.

[13] Rosten H., Spalding D.B., The PHOENICS Beginners Guide, CHAM Ltd., London, 1987.

[14] Spalding D.B., The PHOENICS Encyclopedia, CHAM Ltd., London, 1994.

[15] Patankar S.V., Numerical Heat Transfer and Fluid Flow, Hemisphere, New York, 1980.

[16] Baskaya S., Gilchrist A., Fraser S.M., Buoyancy-induced flow through a narrow chamber containing an internal heat source: comparison of experimental measurements and numerical simulations, Proc. Instn. Mech. Engrs. Part C, J. Mech. Engrg. Science 210 (1996) 489–498.